



# Natural convection of paramagnetic fluid along a vertical heated wall under a magnetic field from a single permanent magnet

メタデータ	言語: eng 出版者: 公開日: 2020-09-24 キーワード (Ja): キーワード (En): 作成者: Kaneda, Masayuki, Fujiwara, Hiroaki, Wada, Kengo, Suga, Kazuhiko メールアドレス: 所属:
URL	<a href="http://hdl.handle.net/10466/00017054">http://hdl.handle.net/10466/00017054</a>

**Natural convection of paramagnetic fluid along a vertical heated wall under a magnetic field from a single permanent magnet**

Masayuki Kaneda<sup>§</sup>, Hiroaki Fujiwara, Kengo Wada and Kazuhiko Suga  
 Dept. of Mech. Eng., Osaka Prefecture Univ., Sakai, Japan

<sup>§</sup>Correspondence author. Fax: +81 72 2549904 Email: mkaneda@me.osakafu-u.ac.jp

**ABSTRACT**

The natural convection of a paramagnetic fluid is numerically investigated in the presence of a magnetic field from a block permanent magnet. One vertical wall of a cavity is partially heated at a constant heat flux to consider a single vertical heated wall. The permanent block magnet is placed behind the heated wall, of which the magnetic field is numerically obtained. Since the magnetic force is remarkable at edges of the block magnet, the magnetothermal force is also pronounced if the temperature difference exists by wall heating. The overlapping magnetothermal force works to repel the fluid. This results in the heat transfer enhancement near the upper magnet edge, and suppression near the lower magnet edge. The suppressing effect becomes remarkable rather than the enhancing one in cases of large magnetic induction, high wall heat flux, and high magnet elevation to the heated wall.

**KEYWORDS:** Natural convection, Paramagnetic liquid, Vertical heated wall, Magnetothermal force, Magnetic field from permanent magnet

**INTRODUCTION**

The natural convection has been widely studied in terms of the natural ventilation, solar heating systems, cooling of nuclear reactors, thermal storages, crystal growth of molten silicon, etc. Since the removal heat flux in limited area has been increasing due to recent development of devices, the convection control and enhancement has become important.

The advantage of the natural convection is, of course, it does not require any power sources to drive the fluid and heat. To control the natural convection, applying an external force can be a candidate. The Coriolis force can induce secondary flow. The Lorentz force on electro-conducting fluid can suppress the natural convection with the application of a magnetic field. The Electric current can induce electro-osmotic flow. In terms of engineering applications, it is favourable that the external force is in low-cost. In the present study, authors focus on the magnetic force from permanent magnets. The magnetic force applied to every material is defined as follows [1].

$$\mathbf{F}_m = \frac{1}{2} \mu_0 \chi_{vm} \nabla \mathbf{H}^2 = \frac{1}{2} \mu_0 \rho \chi_{mm} \nabla \mathbf{H}^2 = \frac{\rho \chi_{mm}}{2 \mu_0} \nabla \mathbf{B}^2 \quad , \quad (1)$$

where  $\mu_0$  is the magnetic permeability in vacuum,  $\chi_{vm} = \rho \chi_{mm}$  is the volumetric magnetic susceptibility (with  $\chi_{mm}$  being the mass magnetic susceptibility and  $\rho$  the density), and  $\mathbf{H} = \mathbf{B}/\mu_0$  is the magnetic field. This obviously suggests that the magnetic force depends both on the magnetic susceptibility (physical property) and the gradient of the squared magnetic induction ( $\nabla \mathbf{B}^2$ ). The ferromagnetic material (iron, cobalt, nickel, etc.) has a large magnetic susceptibility thus it receives a remarkable magnetic force. On the other hand, the force on paramagnetic (air, etc.) and diamagnetic (water, etc.) materials is negligibly small.

Since the emergence of superconducting magnet, tesla-order magnetic induction has become available. This makes the force on paramagnetic and diamagnetic materials remarkable and various new findings have been reported; the levitation of a water droplet [2], a nitrogen jet [3], magnetoarchimedes effect [4]. The application of the strong magnetic field has been also discussed on the protein crystallization [5], convection enhancement / suppression in Rayleigh-Benard convection of paramagnetic fluid [6], natural

convection inside a cubic enclosure [7], and inside concentric annuli [8]. The magnetic force was found to be comparative to the natural convection by applying strong magnetic field [9].

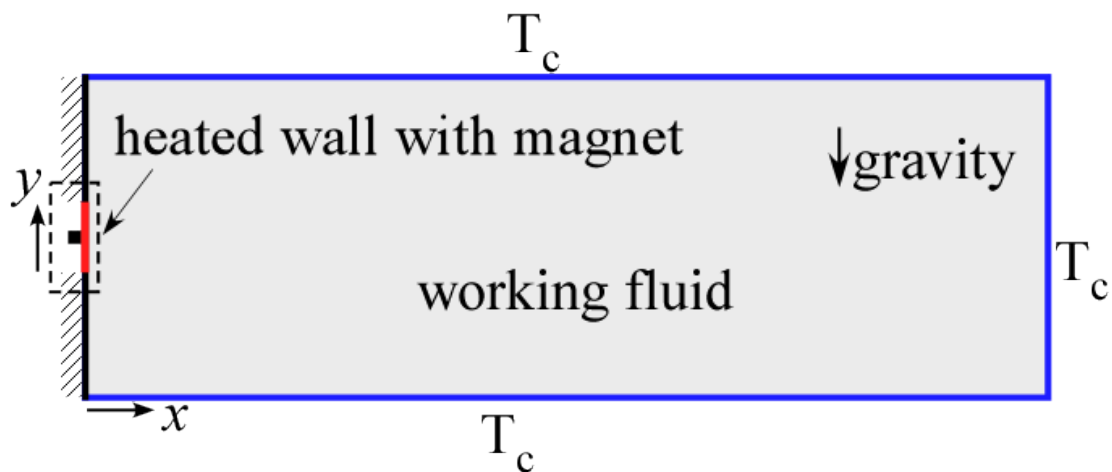
It is known that, the magnetic susceptibility  $\chi$  of the paramagnetic materials depends on the inverse of the absolute temperature, which is called Curie's law. In other words, colder paramagnetic materials can be attracted stronger to the magnet than hotter ones. This can induce the convection similar to the natural convection by density difference. When this force overlaps to the natural convection, the heat transfer is affected, which has been discussed in aforementioned literatures.

In terms of the feasibility of this phenomenon, the convection control by superconducting magnet is too expensive unless the products from the working fluid is more valuable than the running cost of the magnet. Our purpose is to extend the application field with much cheaper magnet cost like permanent magnets. It has been reported that the natural convection of a paramagnetic liquid through a vertical heated duct can be controlled experimentally by block permanent magnets [10]. The natural convection in a cavity filled with oxygen is numerically controlled by permanent magnet [11].

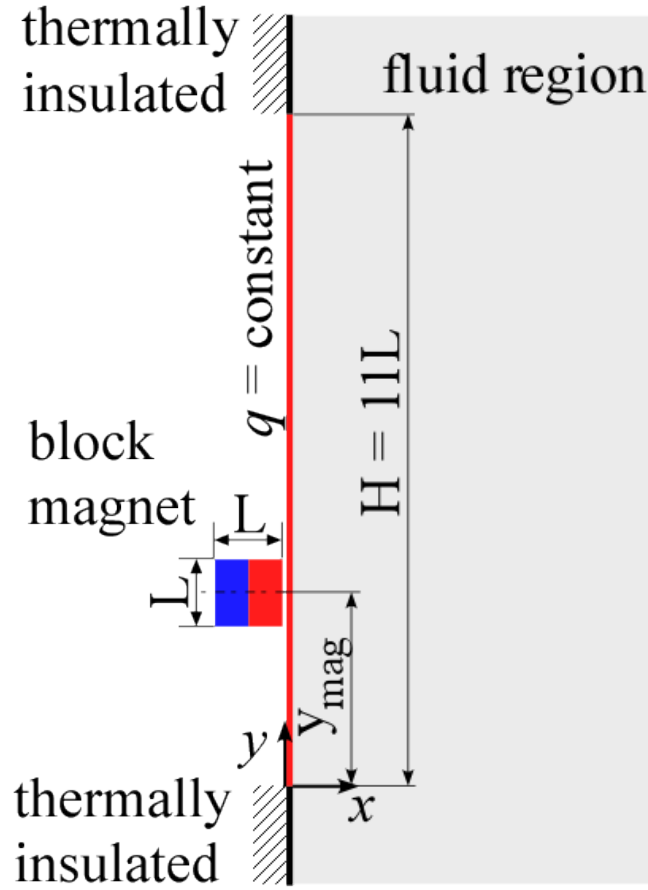
In the present study, the effect of the magnetic field from a block magnet on the natural convection along a vertical wall is numerically investigated. To avoid the unsteady and turbulent convection, one sidewall of the cavity is partially heated to presume the laminar natural convection along the single wall in a sufficiently large cavity.

## COMPUTATIONAL METHOD

**Computational Domain** The computational domain is shown in **Fig. 1(a)** and enlarged image of dashed line area is shown in **Fig.1(b)**. A two-dimensional rectangular enclosure of  $4000(X) \times 1000(Y)$  grid points is considered as the computational domain. The domain is filled with paramagnetic fluid, 15.48 wt. % aqueous solutions of gadolinium nitrate hexahydrate  $[Gd(NO_3)_3 \cdot 6H_2O]$ . This presumes the same solution used in our previous experiment [10]. The physical properties are estimated by the interpolation from the data in Kenjereš et al. [12]. The estimated Prandtl number is 13.0. Sidewalls of the enclosure is kept at constant dimensionless temperature ( $T_c = 1.0$ ) except the left one. The left wall of 220 grid length ( $= H$ : characteristic length) is partially heated at constant heat flux  $q_w$  and other part is thermally insulated. This can presume the natural convection along the heated vertical wall. A single block magnet which side length of 20 grids ( $= L$ ) is placed behind the heated wall ( $=$  left of the left sidewall) with a gap of 3 grids.



(a) Computational domain



(b) Detail of heated wall with magnet (dashed line area in (a))  
**Fig. 1** Schematic model of computation.

**Lattice Boltzmann Method with Magneto-thermal Force** The heat and fluid flow is simultaneously solved by the lattice Boltzmann method (LBM). In the present study, two-dimensional nine-discrete velocity (D2Q9) model is employed, which is illustrated in **Fig. 2**. Two distribution functions are respectively employed for the density  $f_\alpha$  and the thermal energy  $g_\alpha$  to solve the heat and fluid flows. The time evolution equations of both distribution functions at the lattice site  $r$  and time  $t$  are as follows in the single-relaxation-time BGK model.

$$f_\alpha(r + e_\alpha \delta t, t + \delta t) = f_\alpha(r, t) - \frac{\delta t}{\tau_f + 0.5\delta t} (f_\alpha(r, t) - f_\alpha^{eq}(r, t)) + \frac{\tau_f}{\tau_f + 0.5\delta t} F_\alpha \quad (2)$$

$$g_\alpha(r + e_\alpha \delta t, t + \delta t) = g_\alpha(r, t) - \frac{\delta t}{\tau_g + 0.5\delta t} (g_\alpha(r, t) - g_\alpha^{eq}(r, t)) \quad (3)$$

The superscript  $eq$  represents the equilibrium state. The discrete vector is  $e_\alpha$ .  $\tau_f$  and  $\tau_g$  are the relaxation times for  $f_\alpha$  and  $g_\alpha$ , respectively. In the density distribution function (Eq.(2)), external forces due to the buoyancy  $F_g$  and magneto-thermal forces  $F_m$  are considered. The expression of the external force is referred to He et al. [13].

$$F_\alpha = \frac{(F_g + F_m) \cdot (e_\alpha - u)}{RT_0} f_\alpha^{eq} \quad (4)$$

Where,

$$F_g = -\beta\rho_0(T - T_0)g \quad (5)$$

$$F_m = -\frac{\beta\rho_0\chi_0}{2\mu_m}C(T - T_0)\nabla b^2 \quad (6)$$

These suggest followings. The buoyancy force works due to temperature difference modelled by the Boussinesq approximation. The magnetothermal force depends on the magnetic susceptibility  $\chi$ , the temperature difference from the reference temperature, and the local gradient of the squared magnetic induction. The derivation of the magnetothermal force is referred from Kaneda et al. [14].

The macroscopic parameters are related to density distribution functions and relaxation times as follows.

$$\rho = \sum_{\alpha} f_{\alpha}, \quad \rho u = \sum_{\alpha} f_{\alpha} e_{\alpha} + 0.5F_{\alpha}, \quad p = \frac{1}{3}\rho, \quad \nu = \frac{1}{3}\tau_f, \quad T = \sum_{\alpha} g_{\alpha}(r, t), \quad D = \frac{1}{3}\tau_g \quad (7-12)$$

Where,  $D$  is the thermal diffusivity.

The heat flux from the wall is given by the modified Rayleigh number of which characteristic length is represented by the heated wall length  $H$ .

$$Ra_H^* = g\beta qH^4 / \lambda D \nu \quad (13)$$

Please note that, dimensionless computational parameters of  $Pr$  and  $Ra_H^*$  are consisted by the aforementioned dimensionless physical property due to the manner of LBM.

The dimensionless magnetic induction  $\gamma$  is defined as follows,

$$\gamma = \chi_{mm} b_0^2 / (g\mu_0 H) \quad (14)$$

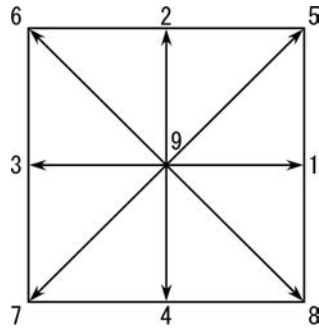


**Fig. 2** Discrete velocity vectors in D2Q9 model.

The computational code is written by CUDA fortran to accelerate the computation and each computation is carried out up to attain the steady state convection.

**Boundary and Initial Conditions** The wall-fluid boundary is considered as half-way bounce-back scheme. The non-slip boundary condition is employed at all enclosure wall. For the thermal boundary conditions, constant dimensionless temperature of  $T_c = 1.0$  is applied to the enclosure walls except the left sidewall. The left sidewall of 220 grid length is heated at a constant heat flux of  $\partial T / \partial X = -1.0$ , and the rest of left sidewall is thermally insulated. These Dirichlet and Neumann thermal boundary conditions are attained by the method of Yoshida and Nagaoka [15].

The initial condition of the computation is that, the fluid is static, the fluid temperature is set at  $T = T_c = 1.0$ , and no magnetic field is applied to the working fluid.

For the natural convection along a vertical heated plate, one may think that the computational domain with free inflow and outflow boundaries (open boundary) at the top and bottom walls can satisfy the situation. However, such boundary conditions are not properly satisfied by LBM due to the poor consideration of incoming distribution function values. Therefore in the present study, a large computational domain at constant temperature is prepared.

**Magnetic Field** The magnetic field from block magnets is numerically obtained by a free software FEMM [16] which solves two-dimensional static magnetic field by finite element method. In this study, magnetic field from square block permanent magnet is numerically obtained.

The obtained magnetic field is shown in **Fig. 3**. In the simulation, the magnetic permeability was set to  $1.26 \times 10^{-6} \text{ mkg}/(\text{s}^2\text{A}^2)$  (air) and  $1.32 \times 10^{-6} \text{ mkg}/(\text{s}^2\text{A}^2)$  (Nd-Fe-B magnet with 40 MGOe), and the Robin condition was applied at the boundary in the computational domain (mixed boundary condition). The magnetic field symmetrically starts from N-pole and converged to S-pole.

The obtained magnetic field is implemented to **Eq. (6)** for the magnetothermal force applied to the natural convection heat and flow flows. In the numerical simulations, the magnetic fields are presumed at arbitral relative elevations to the heated wall, which is defined as  $y_{\text{mag}}$ .

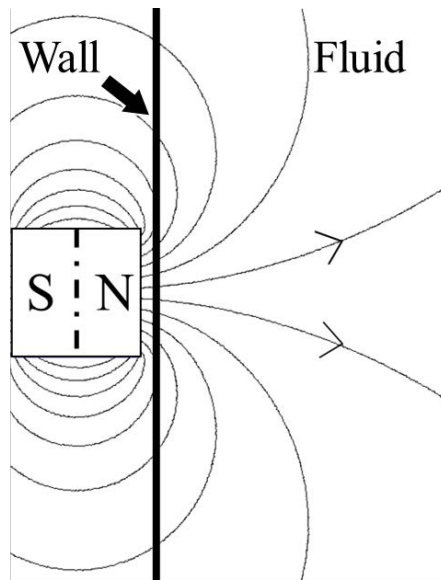


**Fig. 3** Magnetic field from a single block magnet.

**Computational Conditions and Dimensional Value** The parameters of the computations are  $\text{Pr} = 13.0$ ,  $\text{Ra}_H^* = 10^6 - 10^7$ ,  $\gamma = 0-0.3$ , and the magnet location  $y_{\text{mag}} = -0.5L - 6.5L$  where  $L$  represents the magnet side length. The dimensional values of physical property at 293K are estimated from the data in Kenjereš et al. [12]. The thermal diffusivity is  $1.02 \times 10^{-7} \text{ m}^2/\text{s}$ , the kinematic viscosity  $1.30 \times 10^{-6} \text{ m}^2/\text{s}$ , etc. The magnetic susceptibility measured by a magnetic balance is  $1.205 \times 10^{-7} \text{ m}^3/\text{kg}$  [10]. If the length of the heated wall is presumed as 0.11m, corresponding heat flux is  $1.5 \text{ W}/\text{m}^2$  ( $\text{Ra}_H^* = 10^7$ ) and 1.06 Tesla ( $\gamma = 0.1$ ). Since we avoided the unsteady convection, the  $\text{Ra}_H^*$  is limited up to  $10^7$ .

## RESULTS AND DISCUSSION

**Validation of Heat Transfer without Magnetic Field** The natural convection along the heated vertical wall is evaluated. **Fig. 4** shows local Nusselt number versus local modified Rayleigh number along the heated region. The definitions of these dimensionless values are,

$$Nu_{local} = qy/\lambda = \left| -\lambda \frac{\partial T}{\partial x} y \right| / (T_{wall} - T_0) \quad (15)$$

$$Ra_{local}^* = g\beta qy^4 / \lambda D\nu. \quad (16)$$

As shown in the figure, the obtained local Nusselt number agrees very well with the reference data [17]. This suggests that, the present computational scheme has enough validity and the heat transfer characteristic along the heated wall in this large cavity can be regarded as the natural convection along a single vertical heated plate.

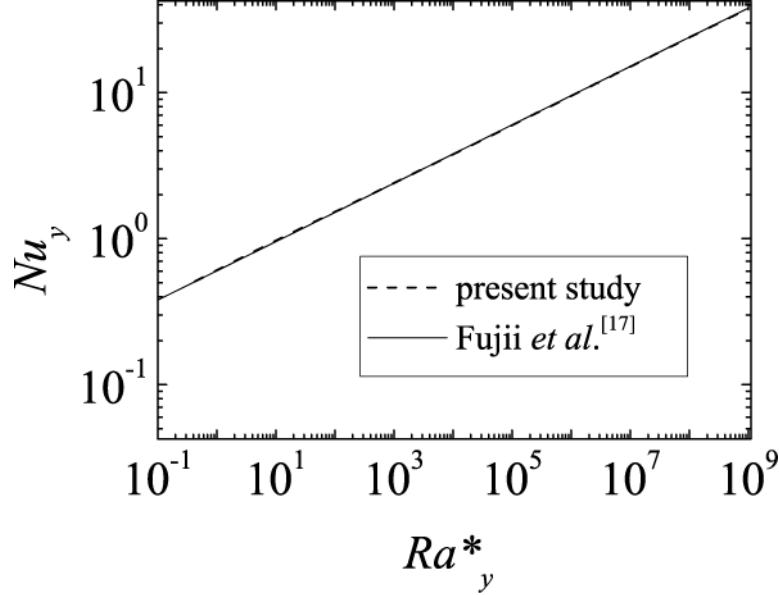


**Fig. 4** Local Nusselt versus modified Rayleigh number along the heated wall without magnetic field.

**Magnetothermal Convection without Gravity** To understand the effect of the magnetothermal force, the induced convection only by the magnetothermal force is investigated. In the present simulation, the gravity acceleration is neglected and the magnet is placed so that its center coincides with the center of the heated wall. **Fig.5** shows the magnetic force component  $\nabla \mathbf{b}^2$ , the magnetothermal force and resulted heat and fluid flow. Since the magnetic field is dense near the magnet edges, the  $\nabla \mathbf{b}^2$  becomes large and strong attractive force works (**Fig.5(a)**). As **Eq.(6)** suggests, since the magnetothermal force is induced by the temperature difference from the reference temperature, the force is directed outward from the magnet when the wall is heated (**Fig.5(b)**). The force induces the flow symmetrically and the temperature field is correspondingly affected(**Fig.5(c)**). The flow has two vortices and the local temperature becomes low around the magnet. These can summarize that the magnetothermal convection by a block magnet induces circulation flows around each edge without gravity, which may be applicable in microgravity field.

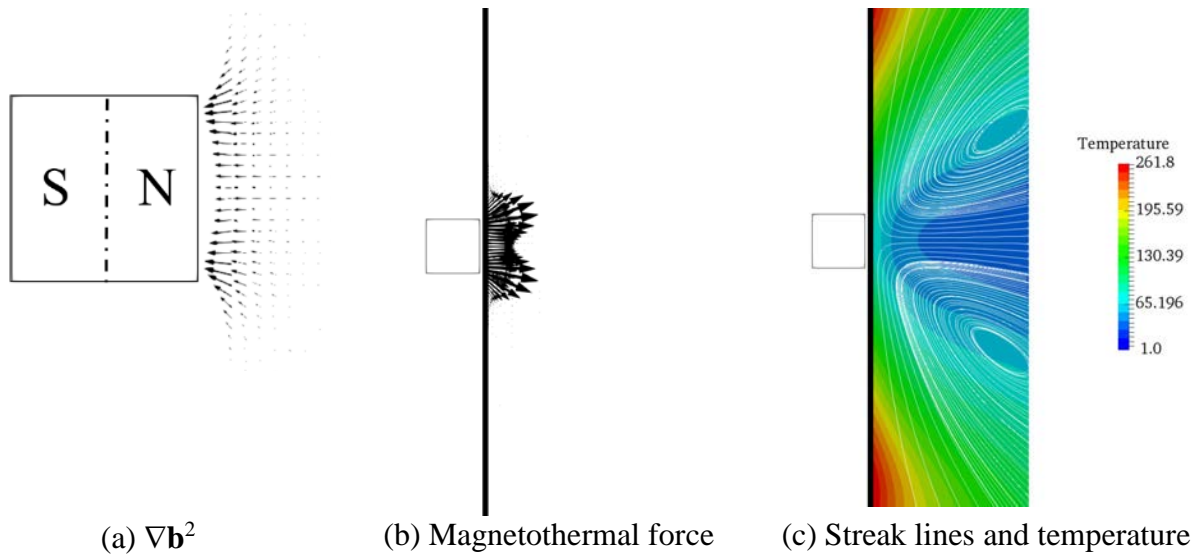


**Fig.5** Magnetothermal convection from a block magnet in the absence of the gravity at  $\gamma Ra_H^* = 5.0 \times 10^5$ .

**Natural Convection with Magnetothermal Force** In the presence of the gravity, the resulted flow is induced both by the buoyancy and magnetothermal force. In this section, the fundamental effect of the magnetothermal force on the natural convection is investigated. **Fig.6** shows the magnetothermal force, and resulted heat and fluid flow. The buoyant and magnetothermal forces depend on the local temperature as **Eqs.(5)** and **(6)** suggests. The combined force is directed outwards from the magnet similar to **Fig.5(b)**. Therefore, the upward flow driven by the buoyancy detours near the bottom magnet edge and it recovers again above the top magnet edge. This tendency is similar to the case in forced convection in a pipe [18], where in front of the electric coil (=magnet) and behind it. The present result suggests that, the magnetic force near the magnet edge plays an important role on the effect when a block permanent magnet is employed for the system.

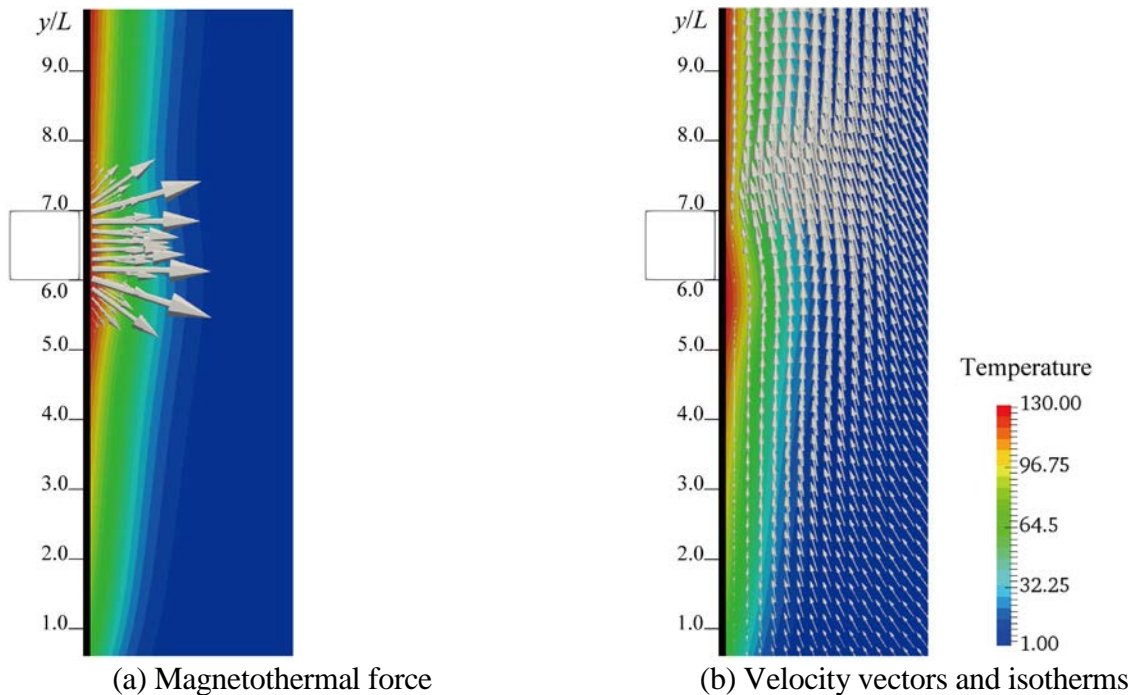


**Fig.6** Magnetothermal force and resulted velocity field and isotherms at  $Ra_H^* = 10^6$ ,  $\gamma = 0.3$ , and  $y_{mag} = 6.5L$ .

Schematic illustration of the magnetothermal force under the gravity field is shown in **Fig.7**. The magnetic attracting force is directed to the magnet. The magnetothermal force is resulted due to temperature difference along the  $\nabla b^2$  vector. In the present case, temperature near the magnet is higher than that of the bulk region, thus the magnetothermal force is in opposite direction against the magnetic force. In the gravity field, the buoyant force is induced also due to the temperature difference and it overlaps to this magnetothermal force. Consequently, the combination force of magnetothermal force and buoyant force applies to the working fluid. Near the top magnet edge, the force accelerates the upward flow. In contrast, near the bottom magnet edge, the force becomes weak than the buoyant force. Please note that, in the absence of the temperature difference, neither buoyancy nor magnetothermal force is induced. For example, if the lower half of the magnet is out of the heated wall, the force near the bottom magnet edge is not induced.

Since the heat and fluid flow is affected by the magnetothermal force by the block magnet, heat transfer is also affected. It is discussed in the following section in terms of the relative location of the magnet to the heated wall, the applied magnetic induction and given heat flux from the wall.

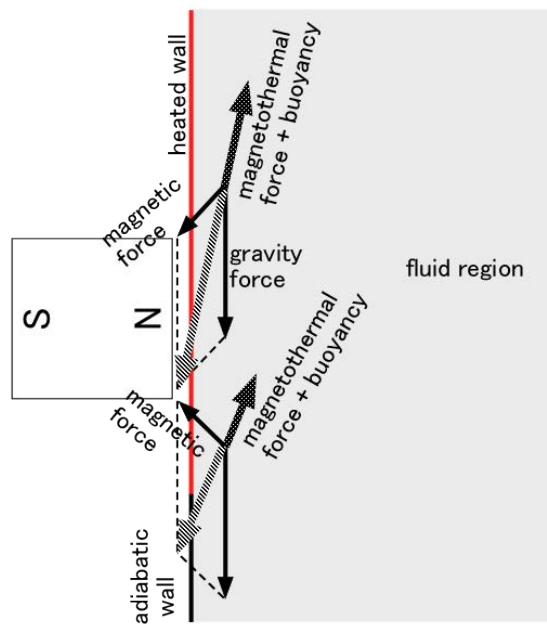


**Fig.7** Schematic model of force applied to the fluid along the heated wall.

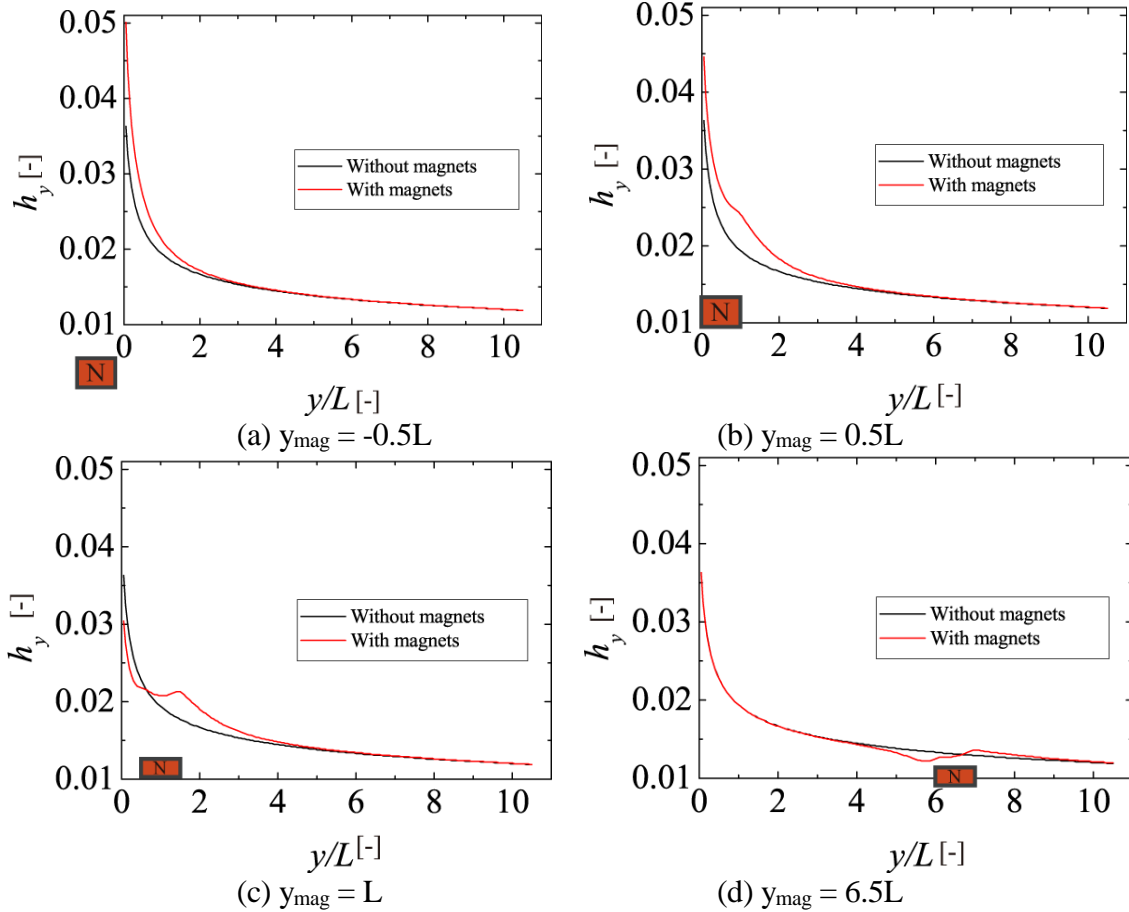
**Effect on the local heat transfer coefficient** To discuss the effect of the applied magnetic field, the local heat transfer coefficient is estimated. The definition is below.

$$h = \frac{q}{T_{wall} - T_c} \quad (17)$$

Since the heat flux  $q$  and temperature  $T$  are in dimensionless form, the obtained heat transfer coefficient is also dimensionless value.

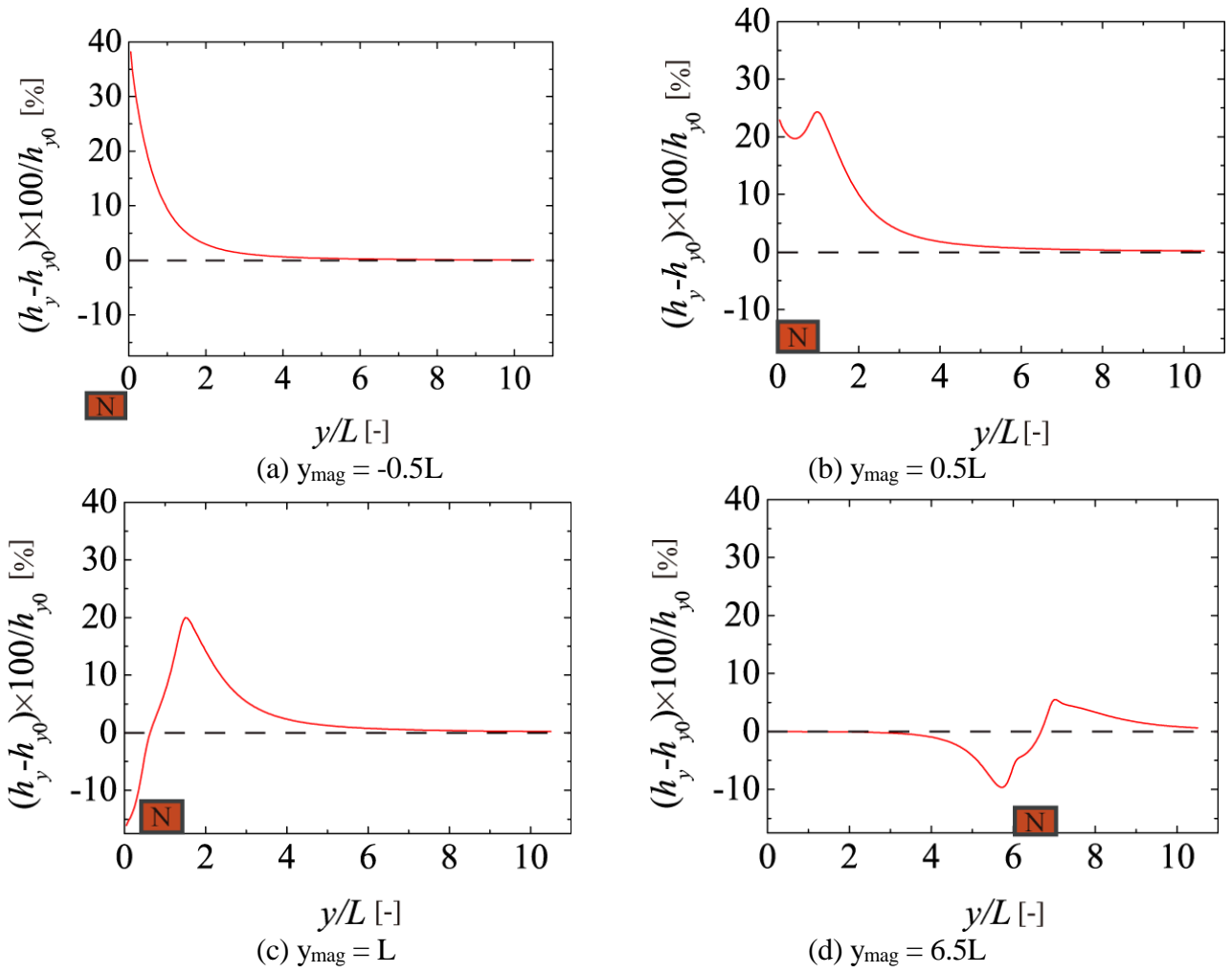
**magnet elevation** The local heat transfer in the presence of the magnetic field from the block magnet of different magnet elevations is shown in **Fig.8**. The abscissa is normalized by the magnet side length  $L$  for a better representation. When the magnet is placed at low elevation, that is, the magnet upper side coincides the heater's bottom (**Fig.8(a)**), the magnetothermal force enhances the local heat transfer around the magnet. This is because that the force near the upper magnet edge becomes remarkable due to the presence of temperature difference and force near the lower magnet edge is negligibly small due to little temperature rise. As the magnet is placed at higher elevation, the magnetothermal force near the bottom magnet edge additionally emerges due to the presence of the temperature difference. In case

where the magnet bottom is aligned to the heater bottom (**Fig.8(b)**), the enhancement near the top magnet edge still overcomes the suppression near the bottom magnet edge. In **Fig.8(c)**, the suppression is observed from the heater bottom to a bit below of the magnet center. When the magnet is placed at much higher elevation (**Fig.8(d)**), the suppression effect obviously surpasses the enhancement effect. Therefore, it can be concluded that, the suppression/enhancement depends largely on the relative magnet elevation to the heated wall.



**Fig.8** Local heat transfer coefficient along the heated wall at difference magnet elevation. Common parameters are  $Ra^*_H = 10^7$  and  $\gamma = 0.1$ .

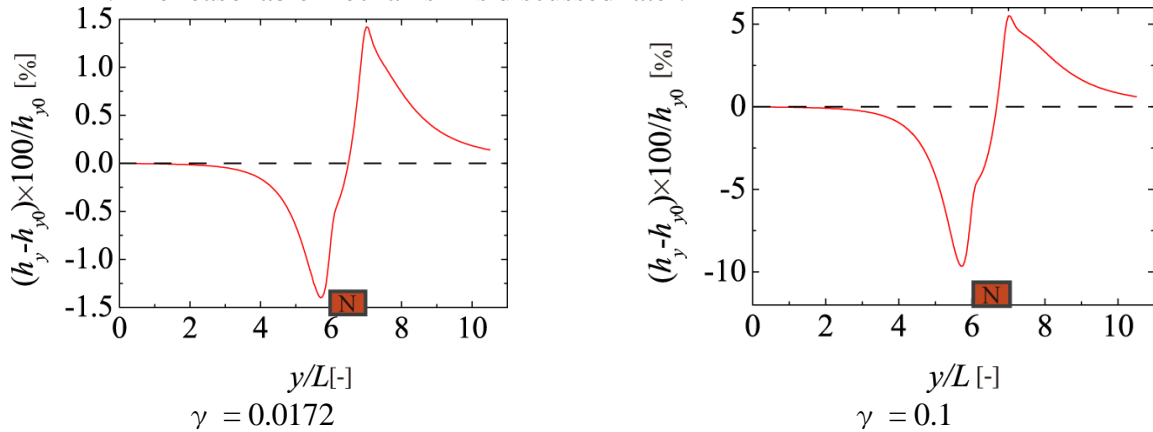
The suppression/enhancement effect is further evaluated. The deviation of local heat transfer coefficient from no-magnetic field case ( $\gamma = 0$ ) is plotted in **Fig.9**. As expected, when the magnet upper edge location coincides the heater bottom, only the enhancement is observed to  $y/L \cong 3.0$  (**Fig.9(a)**). In case that the bottom magnet edge is aligned to the heater bottom (**Fig.9(b)**), the enhancement appears above the top magnet edge ( $y/L > 1.0$ ), and the enhancement becomes weak below it. When both magnet edges are covered by the heating area, both the enhancement near the top magnet edge and suppression near the bottom magnet edge occur (**Figs.9(c), 9(d)**). Especially, the suppression becomes the same magnitude as that of the enhancement if the magnet is placed far away from the heater bottom (**Fig.9(d)**).



**Fig.9** Local heat transfer deviation from no-magnetic case at difference magnet elevation. Common parameters are  $Ra^*_H = 10^7$  and  $\gamma = 0.1$ .

**magnetic induction** In the following discussion, since the fundamental mechanism have clarified, the effect is evaluated by the deviation from the no-magnetic case for the convenience.

The magnetic induction is given by the dimensionless number  $\gamma$ . The effect of  $\gamma$  on the heat transfer along the heated wall is shown in **Fig.10**. In cases investigated, the effect of the magnetic induction is enhanced at larger value of  $\gamma$ . Interestingly, when both suppression and enhancement exists such as high magnet elevations, the suppression effect becomes more remarkable than the enhancement effect as  $\gamma$  increases. The reasonable mechanism is discussed later.



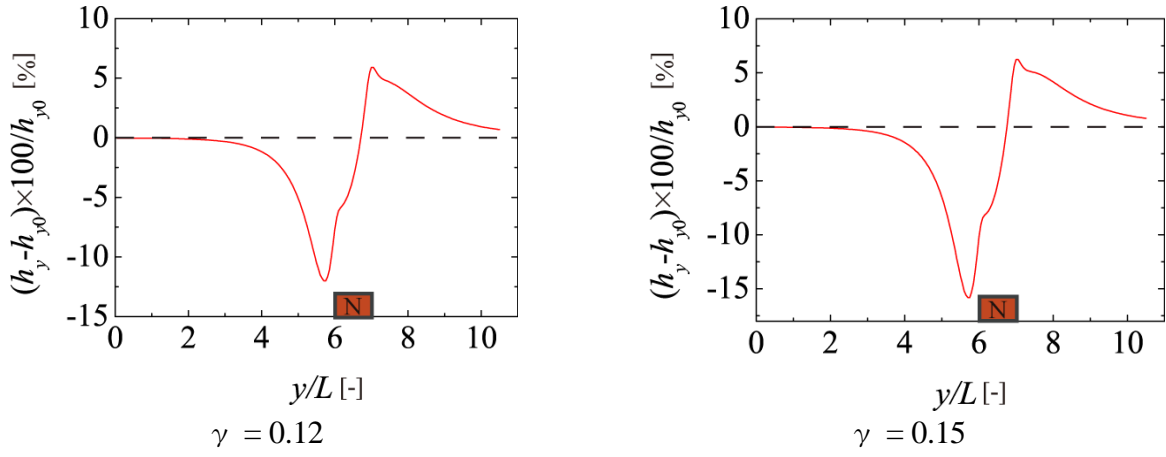


**Fig.10** Local heat transfer deviation from no-magnetic case with difference magnetic induction. Common parameters are  $Ra_H^* = 10^7$  and  $y_{mag} = 6.5L$ .

**wall heat flux** The magnitude of the heat flux from the wall is represented by the modified Rayleigh number  $Ra_H^*$ , of which the characteristic length is the length of heated wall  $H$ . The effect at different  $Ra_H^*$  is shown in **Fig.11**. By increasing the wall heat flux, both the buoyant force and magnetothermal force become strong. Same as in the previous section, the suppression effect becomes more remarkable than the enhance effect when the heat flux increases.

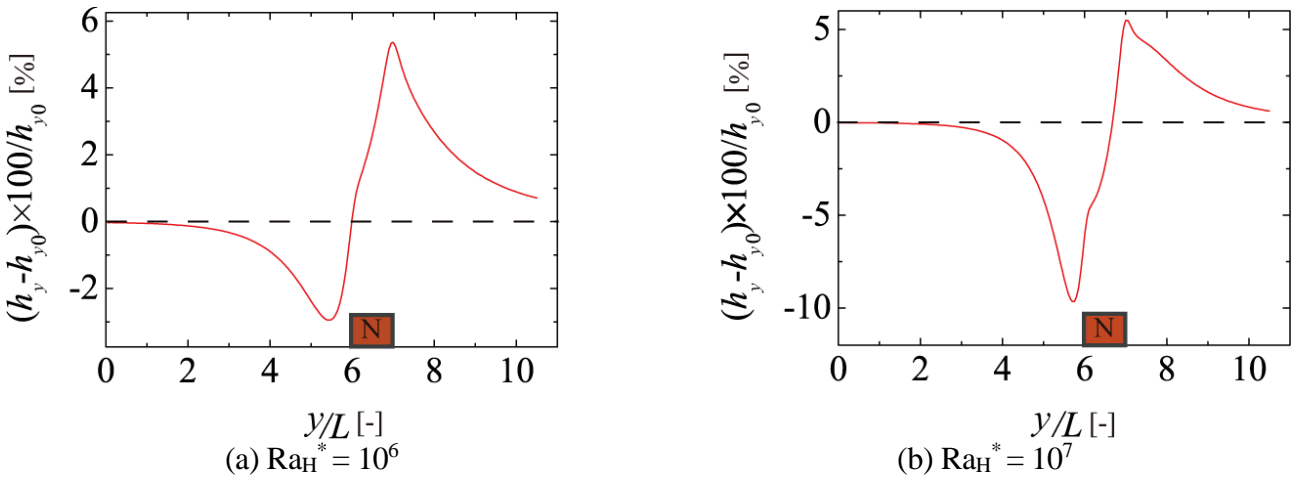


**Fig.11** Local heat transfer deviation from no-magnetic case with difference magnetic induction. Common parameters are  $\gamma = 0.1$  and  $y_{mag} = 6.5L$ .

**why is the suppression effect pronounced?** In cases of the higher magnet elevation and strong magnetothermal force such as strong magnetic induction and high wall heat flux, the suppression effect becomes more remarkable than the enhancement effect. This implies that the magnetothermal force near the bottom magnet edge becomes stronger than that near the top magnet edge. To confirm the hypothesis, the magnitude of the magnetothermal force is shown in **Fig.12**. As shown at low  $Ra_H^*$ , the profile seems symmetric and similar for both magnetic inductions. In these cases, the enhancement effect is more distinguished than the suppression. The same tendency is found at high  $Ra_H^*$  with weak magnetic induction (**Fig.12(b)** left). However, by the increased magnetic induction (**Fig.12(b)** right), the profile becomes a bit asymmetry, especially adjacent to the bottom edge. Since the magnetothermal force radiates from the magnet, the force near the bottom magnet edge interrupts the heat and fluid flows. This blocking effect of heat and fluid flow induces the temperature rise near the bottom magnet edge. This temperature rise enhances the magnetothermal force near the bottom magnet edge again.

Finally, the stable profile near the bottom magnet edge is formed by balancing the buoyancy and magnetothermal force.

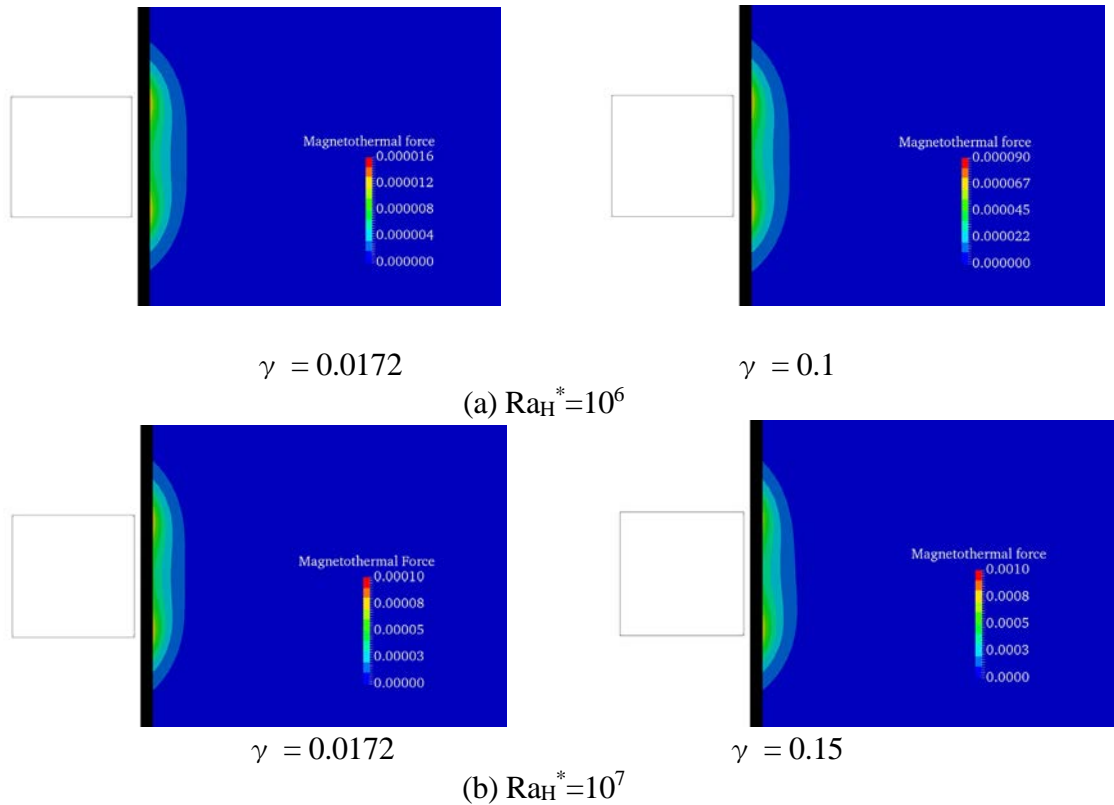


**Fig.12** Magnitude of magnetothermal force at  $y_{mag} = 6.5L$ .

## CONCLUSION

The effect of a magnetic field by a block magnet on the natural convection of a paramagnetic fluid along the heated wall is numerically investigated. It is confirmed that, the magnetothermal force by a block magnet is directed to repel from the magnet if the magnet is behind the heater. This results in the enhancement of the local heat transfer near the top magnet edge, and in contrast, the magnetothermal force suppresses the convection near the bottom magnet edge. When the magnetothermal force becomes stronger such as high magnetic induction and/or high wall heat flux, the suppression effect becomes more remarkable than the enhancement effect due to the temperature rise near the bottom magnet edge. Cases of the high magnet elevation to the heated wall also induces strong magnetothermal force and the suppression effect is pronounced. Therefore, the magnetic field near the bottom magnet edge has a blocking effect on the buoyant flow depending on the magnetic induction, heat flux, and magnet elevation.

The present numerical study shows the fundamental characteristic of magnetothermal force on natural convection, and local heat transfer can be controlled by a block magnet. The estimated magnetic induction of  $\gamma=0.1$  is 1.06 Tesla which is a bit stronger than available permanent magnets. The magnetic force can be enhanced not only by the development of magnet material but also the multiple magnet arrangements. Since the heat transfer enhancement can be expected by placing the magnet at heater bottom, this study can contribute to the heat exchanging devices such as fin plate, micro channel, etc.,

## ACKNOWLEDGEMENT

This study is partially supported by MEXT and a Grant-in-aid for Scientific Research (C) No. 18K03988. The authors would like to thank M. Sugimoto for technical assistance with the simulation.

## REFERENCES

- [1] Carruthers, J.R., Wolfe, R.: Magnetothermal convection in insulating paramagnetic fluids, *Journal of Applied Physics*, 39, 5718-5722 (1968).
- [2] Ikezoe, Y., Hirota, N., Nakagawa, J., Kitazawa, K.: Making Water Levitate. *Nature*, 393, 749-750 (1988).
- [3] Wakayama, N.I.: Behavior of Gas Flow under Gradient Magnetic Fields. *J. Appl. Phys.*, 69, 2734-2736 (1991).
- [4] Kitazawa, K., Ikezoe, Y., Uetake, H., Hirota, N.: Magnetic field effects on water, air and powders. *Physica B: Condensed Matter*, 294, 709-714 (2001).
- [5] Maki S., Ataka M., Tagawa T., Ozoe H., Mori W.: Natural Convection of a Paramagnetic Liquid Controlled by Magnetization Force. *AIChE Journal*, 51, 1096-1103 (2005).
- [6] Braithwaite, D., Beaugnon, E., Tournier, R., Magnetically Controlled Convection in a Paramagnetic Fluid, *Nature*, 354, no. 6349, 134–136 (1991).
- [7] Kaneda M., Noda, R., Tagawa, T., Ozoe, H., Lu, S-S, Hua, B.: Effect of inclination on the convection of air in a cubic enclosure under both magnetic and gravitational fields with flow visualization, *J. Chemical Engineering of Japan*, 37, 2, 338-346 (2004).
- [8] Wrobel W.A., Fornalik-Wajs E. and Szmyd J.S.: Analysis of the Influence of a Strong Magnetic Field Gradient on Convection Process of Paramagnetic Fluid in the Annulus between Horizontal Concentric Cylinders, *J. Phys: Conf. Ser.*, 395, 012124 (2012).
- [9] Bednarz T., Tagawa T., Kaneda M., Ozoe H. and Szmyd J.S.: Magnetic and Gravitational Convection of Air with a Coil Inclined around the X Axis, *Num. Heat Trans.*, 46, 99-113 (2004).
- [10] Kaneda, M., Nazato, K., Fujiwara, H., Wada, K., Suga, K., Effect of magnetic field on natural convection inside a partially-heated vertical duct: Experimental study, *International Journal of Heat and Mass Transfer*, 132, 1231-1238 (2019).
- [11] Song, K.W., Tagawa, T., Thermomagnetic convection of oxygen in a square enclosure under nonuniform magnetic field, *International Journal of Thermal Sciences*, 125, 52-65 (2018).
- [12] S. Kenjereš, L. Pyrda, W. Wrobel, E. Fornalik-Wajs, J.S. Szmyd, Oscillatory states in thermal convection of a paramagnetic fluid in a cubical enclosure subjected to a magnetic field gradient, *Phys. Rev. E*. 85 (2012) 046312.
- [13] He X., Chen S. and Doolen G.D.: A Novel Thermal Model for the Lattice Boltzmann Method in Incompressible Limit". *J. Comput. Phys.*, 146, 282-300 (1998).
- [14] Kaneda M., Kano H. and Suga K.: Development of Magneto-Thermal Lattice Boltzmann Heat and Fluid Flow Simulation. *Heat Mass Trans.*, 51, 1263-1275 (2015).
- [15] Yoshida, H., Nagaoka, M., Multiple-relaxation-time lattice Boltzmann model for the convection and anisotropic diffusion equation, *Journal of Computational Physics*, 229, 7774-7795 (2010).
- [16] <http://www.femm.info/wiki/Documentation/>
- [17] T. Fujii and M. Fujii, The dependence of local Nusselt number on Prandtl number in the case of free convection along a vertical surface with uniform heat flux, *International Journal Heat and Mass Transfer* 19, 121-122 (1976).
- [18] Kaneda, M., Tsuji, A., Ooka, H., and Suga, K.: Heat transfer enhancement by external magnetic field for paramagnetic laminar pipe flow. *International Journal of Heat and Mass Transfer*, 90, 388-395 (2015).